Maximum Measurable Distances for a Single-Mode Optical Fiber Fault Locator Using the Stimulated Raman Scattering (SRS) Effect

YASUJI MURAKAMI, MEMBER, IEEE, KAZUHIRO NOGUCHI, FUMIHIRO ASHIYA, YUKIYASU NEGISHI, AND NOBUYA KOJIMA, MEMBER, IEEE

Abstract—**Maximum measurable distances for a single-mode optical fiber fault locator using the stimulated Raman scattering effect were calculated. Calculations were carried out on the assumption that the light source is an Nd:YAG laser operating at 1.06 μm and the photodetector is a germanium avalanche photodiode (Ge-APD). The first to the seventh Stokes lights can be detected by the Ge-APD. Calculations show that a break can be measured in an up to 165 km long ultra-low-loss single-mode fiber.**

I. Introduction

DUE to recent attainment of low-loss optical fibers in the 1.0-1.8 μm spectral region, long repeater spacing optical communication systems, such as a submarine optical cable transmission system, have been developed [1]-[3]. In order to realize the long span optical fiber cable systems, however, it is necessary to develop fiber fault location technology. The optical time domain reflectometry (OTDR) is an effective technique for locating fiber breaks and for determining the loss distribution along the fiber [4], [5]. Several studies have reported the OTDR in a single-mode fiber [6], [7]. In these methods, however, it is difficult to locate breaks in a more than 50 km long single-mode fiber because fiber input power is limited to be less than 10 W in order to prevent optical damage to the directional coupler and photodiode.

Recently, a new fault location method for an ultra-long fiber was proposed [8], [9]. It uses Stokes lights, which are generated in a measured fiber by the stimulated Raman scattering (SRS) effect, as probing optical pulses. In this method, low-loss and low-crosstalk separation between the input optical pulse and the backscattered light pulses can be realized by an optical wavelength filter because wavelengths of the input and the backscattered lights are different. Furthermore, since the optical wavelength filter is not damaged by high power optical pulses, it is possible to insert the high power pulses into the fiber and to generate the higher order Stokes lights in the 1.5-1.6 μm wavelength region, which are most advantageous for the fault location because the fiber loss is lowest at 1.55 μm. Therefore, this method seems to have an advantage of locating breaks in ultra-long optical fiber.

This paper reports calculations of maximum measurable distances for the single-mode fiber fault locator using the SRS effect. Calculations were carried out on the assumption that the light source is a Q-switched Nd:YAG laser operating at 1.06 μm and the photodetector is a germanium avalanche photodiode (Ge-APD). As a result, it is shown that a break can be measured in an up to 165 km long ultra-low-loss single-mode fiber.

Manuscript received March 1, 1982; revised May 11, 1982.

The authors are with the Ibaraki Electrical Communication Laboratory, Nippon Telegraph and Telephone Public Corporation, Tokai, Ibaraki, Japan.

II. Principle of the Fault Locator Using SRS

Measurement principle for the fault locator using SRS is shown in Fig. 1. Output light pulses from the Q-switched Nd:YAG laser operating at 1.06 μm are reflected by the optical filter and are inserted into the optical fiber to be analyzed. When high power light pulses, with more than 10 W peak power, are inserted into a single-mode fiber, the pulses generate the first Stokes light pulses due to the SRS effect, whose optical frequency is shifted by 450 cm^{-1} shorter than the pumping pulses [9]. These Stokes light pulses generate higher order Stokes light pulses as they propagate along the fiber. The generated Stokes lights suffer from Rayleigh scattering. Some of them become backscattered light and reach the optical filter through the fiber input end. The optical filter has characteristics wherein lights whose wavelengths are shorter than 1.1 μm are reflected and lights whose wavelengths are longer than 1.1 μm pass through. Therefore, only the Stokes lights pass through the filter and reach the Ge-APD. Since any pumping pulse, which is Fresnel reflected at the fiber input end, is reflected by the optical filter, excess APD photocurrent due to this light is removed.

Fig. 2 shows the transmittance of the optical filter and the quantum efficiency of the Ge-APD used for the following calculations. Their characteristics are assumed to be ideal. The optical filter transmits lights whose wavelengths are longer than 1.1 μm with 100 percent efficiency. The Ge-APD quantum efficiency is assumed to be 60 percent independent of the wavelength, when the wavelength is shorter than the Ge-APD cutoff wavelength of 1.60 μm. Therefore, only the first to the seventh Stokes lights (first: 1.12 μm, second: 1.18 μm, ··· seventh: 1.60 μm) are detected by the Ge-APD.

III. Stokes Lights Generation in Single-Mode Fibers

In the measurement system mentioned above, the Rayleigh backscattered lights of the Stokes light pulses, generated in a measured fiber, are used as signal lights. Therefore, it is necessary to obtain the Stokes light powers for the received signal-to-noise ratio (SNR) calculations. The following two assumptions are set to simplify the Stokes power calculation.

1) The time waveform for the pumping light pulse is rectangu-

0018-9480/82/1000-1461$00.75

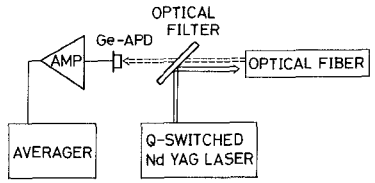

Fig. 1. Block diagram of the setup for the fault locator using SRS.

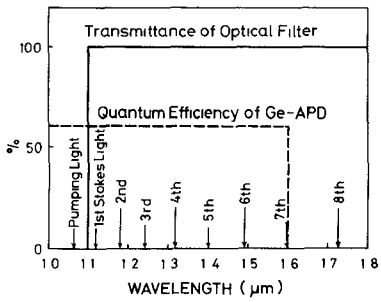

Fig. 2. Optical wavelength filter transmittance and Ge-APD quantum efficiency used for calculations.

lar and its pulse width is longer than the maximum interaction time between the pumping and the Stokes lights.

2) The bandwidth of the Raman gain curve is narrow enough to assume that the Stokes lights are single frequency.

Therefore, the spatial separation between the pumping pulse and the Stokes pulses, due to the fiber dispersion, is neglected, and nonlinear process are calculated with the continuous wave condition.

The 1.06 μm pumping power P_0 and the λ_n μm nth Stokes power $P_n(n = 1, 2, \cdots)$ at z in a single-mode fiber change in accordance with the following equations, as they propagate along the fiber [10]:

$$dP_0/dz + \alpha_0 P_0 = -(g_0/A_0) P_0 P_1 \tag{1}$$

$$dP_n/dz + \alpha_n P_n = (g_{n-1}/A_{n-1}) P_{n-1} P_n - (g_n/A_n) P_n P_{n-1} \tag{2}$$

where α_n, g_n, and $A_n(n = 0, 1, 2, \cdots)$ are fiber loss, Raman gain coefficient, and single-mode fiber effective cross section at each wavelength, respectively.

Fiber loss α_n is the sum of ultraviolet absorption loss $\alpha_{\mathrm{UV},n}$, infrared absorption loss $\alpha_{\mathrm{IR},n}$, Rayleigh scattering loss $\alpha_{R,n}$, waveguide imperfection loss $\alpha_{I,n}$, and OH absorption loss $\alpha_{\mathrm{OH},n}$. Therefore, fiber loss at wavelength λ_n is given by [11]

$$\alpha_n = \alpha_{\mathrm{UV},n} + \alpha_{\mathrm{IR},n} + \alpha_{R,n} + \alpha_{I,n} + \alpha_{\mathrm{OH},n}, \tag{3}$$

$$\alpha_{\mathrm{UV},n} = \frac{15.42\Delta}{4.46\Delta + 60} 10^{-2} \exp\left(-\frac{4.63}{\lambda_n}\right) \quad [\mathrm{dB/km}], \tag{4}$$

$$\alpha_{\mathrm{IR},n} = 7.81 \times 10^{11} \exp\left(-\frac{48.48}{\lambda_n}\right) \quad [\mathrm{dB/km}], \tag{5}$$

$$\alpha_{R,n} = (0.75 + 0.45\Delta)/\lambda_n^4 \quad [\mathrm{dB/km}], \tag{6}$$

$$\alpha_{\mathrm{OH},n} = \alpha_{1.38} \exp\left[-\left(\frac{1.38 - \lambda_n}{0.024}\right)^2\right] + \alpha_{1.38}\left(\frac{2.8}{65}\right) \cdot \exp\left[-\left(\frac{1.24 - \lambda_n}{0.024}\right)^2\right] \quad [\mathrm{dB/km}] \tag{7}$$

where Δ is the relative refractive index difference between core and cladding, $\alpha_{1.38}$ is the OH absorption loss at 1.38 μm. Fiber losses when $\Delta = 0.28$ percent, calculated from (3)-(7), are shown in Fig. 3. Curve (A) is the theoretical value of an ultra-low-loss fiber with $\alpha_I = 0$ dB/km and $\alpha_{\mathrm{OH}} = 0$ dB/km. Curve (B) shows the loss when α_I is 0.15 dB/km, independent from the wavelength, and curve (C) shows the loss when $\alpha_{1.38}$ is 3 dB/km in addition to α_I. In any case, loss becomes lowest at the wavelengths of the sixth and seventh Stokes lights.

The Raman gain varies inversely with wavelength [10]. Since the gain coefficient is 9.2×10^{-14} m/W at 1.064 μm [12], the wavelength dependence of the coefficient becomes

$$g_n = (1.064/\lambda_n)\, 9.2 \times 10^{-14} \quad [\mathrm{m/W}]. \tag{8}$$

If the LP_{01} mode [13] is approximated by a Gaussian value, effective cross section A_n is given by [14], [15]

$$A_n = 2\pi w_n^2, \tag{9}$$

$$w_n = a(0.65 + 1.619/V_n^{3/2} + 2.879/V_n^6) \tag{10}$$

where a is the core radius and V_n is the normalized frequency at λ_n.

Equations (1) and (2) are numerically calculated by the Runge-Kutta method, in which the Stokes power injected at $z = 0$ is assumed to be

$$P_n(0) = h\lambda_n B_{\mathrm{eff},n} \tag{11}$$

where h is Planck's constant, λ_n is the nth Stokes light frequency, and $B_{\mathrm{eff},n}$ is the effective gain bandwidth [16]. The bandwidth is given by

$$B_{\mathrm{eff},n} = \frac{\Delta\nu_R}{2}\left[\frac{\pi\alpha_n A_n}{g_n P_0(0)}\right]^{1/2} \tag{12}$$

where $\Delta\nu_R$ is the full width of the Raman gain and is set to be 300 cm^{-1} [17] in the following results.

Generated Stokes light powers are shown in Fig. 4 versus fiber length. The fiber parameters used in the calculations are 9 μm core diameter and 0.28 percent relative refractive index difference. These values are the most suitable parameters for submarine optical fiber cable [3]. The loss value with $\alpha_I = 0.15$ dB/km and $\alpha_{\mathrm{OH}} = 0$ dB/km, as shown by curve (B) in Fig. 3, is used. Fig. 4(a)-(c) shows the power when the input powers are 50, 60, and 70 W, respectively. When the input power is 50 W, the fifth Stokes light is generated at 16 km, but the sixth Stokes light does not appear. When the power is 60 W, the seventh Stokes light is generated finally, in which the fiber loss is lowest. In the case of 70 W, the eighth Stokes light is generated at 25 km, where the loss is higher than that of the seventh Stokes light. Therefore, the Stokes power at 60 km decreases to a quarter of that when the input power is 60 W.

IV. Maximum Measurable Distance

If the Stokes power at z is $P_n(z)$, the power received by the Ge-APD due to the Rayleigh backscattering at z is given by

$$P = \frac{Wv}{2} \sum_{n=1}^{7} P_n(z)\, \alpha_{R,n} S_n \exp(-\alpha_n z) \tag{13}$$

and the photocurrent by this power is

$$I = \frac{Wv}{2} \sum_{n=1}^{7} \frac{\eta e}{h\nu_n} P_n(z)\, \alpha_{R,n} S_n \exp(-\alpha_n z) \tag{14}$$

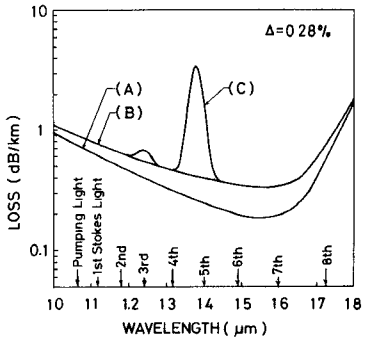

Fig. 3. Fiber losses when $\Delta = 0.28$ percent. Curve (A) is the theoretical value of an ultra-low-loss fiber with $\alpha_I = 0$ dB/km and $\alpha_{OH} = 0$ dB/km. Curve (B) shows the value with $\alpha_I = 0.15$ dB/km and $\alpha_{OH} = 0$ dB/km. Curve (C) shows the value with $\alpha_I = 0.15$ dB/km and $\alpha_{1.38} = 3$ dB/km.

where

W: input pulse width,

v: light velocity in a fiber,

η: Ge-APD quantum efficiency,

e: electron charge.

Backscattering factor S_n is given by [6]

$$S_n = \frac{1}{4}\left(\frac{\lambda_n}{\pi n_1 w_n}\right)^2 \tag{15}$$

where n_1 is the core refractive index.

Received SNR in the OTDR is given by [6]

$$S/N = \frac{(IM)^2}{\left[2e(I+I_d)M^3 + \frac{4FkT_{\text{eff}}}{R}\right]B} \tag{16}$$

where

M: APD multiplication factor,

I_d: APD dark current,

R: APD load resistance,

F: amplifier noise factor,

k: Boltzman factor,

T_{eff}: effective temperature,

B: received bandwidth.

The SNR calculation result for fiber with $2a = 9\ \mu$m, $\Delta = 0.28$ percent, $\alpha_I = 0.15$ dB/ km, and $\alpha_{OH} = 0$ dB/km is shown in Fig. 5, where $M = 7.4$, $I_d = 10^{-7}$ A, $R = 1$ kΩ, $F = 6$ dB, $T_{\text{eff}} = 300$ K, and $B = 20$ MHz are used. The SNR when the input power is 60 W becomes higher than that in the 50 W case because the fiber loss for the seventh Stokes light, which is the final Stokes light at 60 W, is lower than that for the fifth Stokes light in the 50 W case. When the input power is 70 W, the SNR rapidly degrades from 25 km because 1.73 μm eighth Stokes light, where Ge-APD is cutoff, is generated at this point. Therefore, there is optimum input power near 60 W. The 50 dB SNR improvement in the OTDR signal can be realized by the digital averager [5]. For this reason, −45 dB of the received SNR becomes 5 dB, using the averager. This value is assumed to be a measurable limit. The dashed line in Fig. 5 shows SNR = −45 dB.

Measurable distances when the SNR limit is −45 dB are shown in Fig. 6 versus input optical power, where $\alpha_{OH} = 0$ dB/ km and α_I is used as a parameter. The maximum measurable distance becomes 165 km when the input power is 44 W for the case of an ultra-low-loss fiber, as shown by curve (A) in

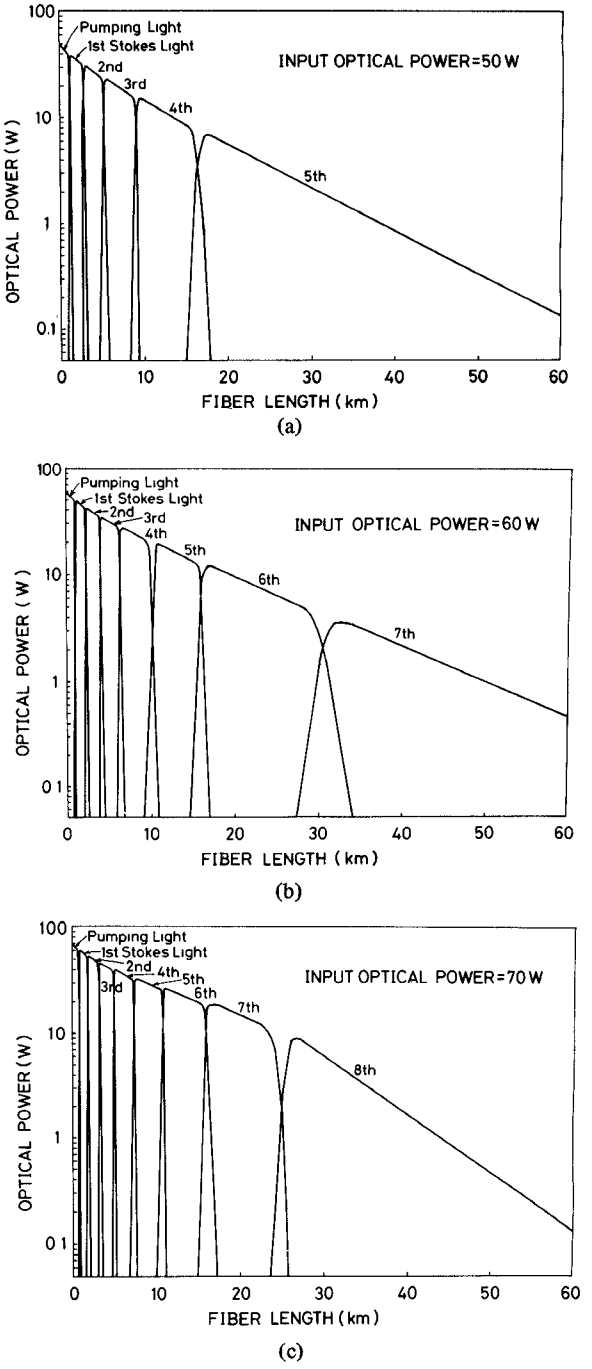

Fig. 4. Generated Stokes powers for $2a = 9\ \mu$m, $\Delta = 0.28$ percent, $\alpha_I = 0.15$ dB/km, and $\alpha_{OH} = 0$ dB/km. Input optical power values are (a) 50 W, (b) 60 W, and (c) 70 W.

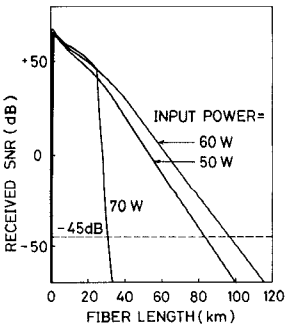

Fig. 5. Received SNR in the fault locator using SRS for a single-mode fiber with $2a = 9\ \mu$m, $\Delta = 0.28$ percent, $\alpha_I = 0.15$ dB/km, and $\alpha_{OH} = 0$ dB/km.

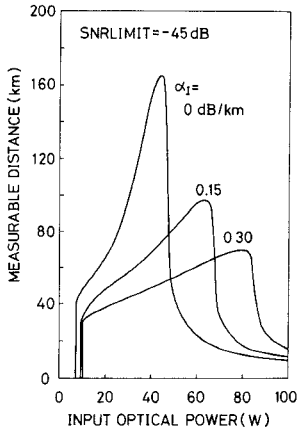

Fig. 6. Measurable distance versus input optical power where $\alpha_{OH} = 0$ dB/km and α_I is used as a parameter.

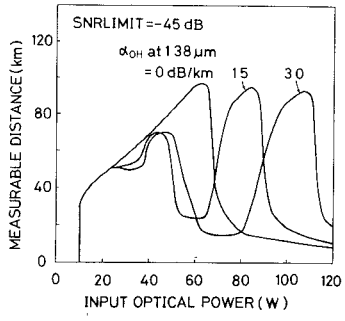

Fig. 7. Measurable distance versus input optical power where $\alpha_I = 0.15$ dB/km and $\alpha_{1.38}$ is used as a parameter.

Fig. 3. If the loss increases, the maximum measurable distance decreases and the optimum input power, at which the measurable distance is maximum, increases. Fig. 7 shows the measurable distance when $\alpha_I = 0.15$ dB/km and $\alpha_{1.38}$ is used as a parameter. If $\alpha_{1.38} = 1.5$ or 3.0 dB/km, there are two peaks of the measurable distance versus input power. These peaks correspond to the cases in which the final Stokes lights are the 1.32 μm fourth Stokes light and the 1.60 μm seventh Stokes light, respectively. The maximum measurable distance, however, is almost constant at 95 km, independent of the OH absorption loss. The reason is that fiber losses at 1.60 μm in the three cases are the same.

If the fiber parameters are different, the effective cross section changes and the interaction length for the Stokes lights changes. As a result, the optimum input power varies. The measurable distances for the different fiber parameters are shown in Fig. 8, where $\alpha_I = 0.15$ dB/km and $\alpha_{OH} = 0$ dB/km. Curve (I) shows the cases where $2a = 9$ μm and $\Delta = 0.28$ percent; curve (II) shows that for $2a = 5$ μm and $\Delta = 0.28$ percent; and curve (III) shows that for $2a = 5$ μm and $\Delta = 0.80$ percent. In the fiber with curve (III) parameters, fiber dispersion becomes zero at 1.55 μm. The optimum input power decreases when the core diameter becomes smaller or the relative index difference becomes larger. This reason is that the effective cross section becomes smaller and the threshold power of the Stokes light generation decreases. If the fiber losses in each case coincide at 1.60 μm, however, the maximum measurable distances become almost the same.

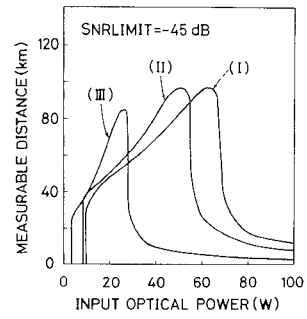

Fig. 8. Measurable distance versus input optical power, where $\alpha_I = 0.15$ dB/km and $\alpha_{OH} = 0$ dB/km. Curve (I) shows the fiber with $2a = 9$ μm and $\Delta = 0.28$ percent. Curve (II) shows the fiber with $2a = 5$ μm and $\Delta = 0.28$ percent. Curve (III) shows the fiber with $2a = 5$ μm and $\Delta = 0.80$ percent.

V. Conclusion

The maximum measurable distance for the single-mode optical fiber fault locator using the SRS was calculated. Calculations were carried out on the assumption that the light source is 1.06 μm Nd:YAG laser and the photodetector is Ge-APD. Fiber loss is considered to be the sum of ultraviolet absorption loss, infrared absorption loss, Rayleigh scattering loss, waveguide imperfection loss, and OH absorption loss. As a result, the following results are obtained.

1) There is an optimum value in the fiber input optical power where, if the fiber is excited with this optimum power, a fiber fault can be located up to 165 km away in an ultra-low-loss fiber.

2) Optimum input power varies with fiber loss and fiber parameters, but the maximum measurable distance is determined by fiber loss at 1.60 μm. The distance decreases as the loss becomes higher.

Acknowledgment

The authors wish to thank Dr. H. Fukutomi and Dr. Y. Kato for their continuous encouragement. They are also indebted to Dr. K. Ishihara for fruitful discussions.

References

[1] E. Iwahashi, "Trends in long-wavelength single-mode transmission systems and demonstrations in Japan," *IEEE J. Quantum Electron.*, vol. QE-17, pp. 890-896, June 1981.

[2] N. Kojima, T. Yabuta, Y. Negishi, K. Iwabuchi, O. Kawata, K. Yamashita, Y. Miyajima, and N. Yoshizawa, "Development and laying results of submarine optical fiber cable," *Appl. Opt.*, Feb. 1982.

[3] N. Kojima, Y. Miyajima, Y. Murakami, T. Yabuta, O. Kawata, K. Yamashita, and N. Yoshizawa, "Studies on designing of submarine optical fiber cable," *IEEE J. Quantum Electron.*, vol. QE-18, pp. 733-740, Apr. 1982.

[4] S. D. Personick, "Photon probe—An optical-fiber time-domain reflectometer," *Bell Syst. Tech. J.*, vol. 56, pp. 355-366, Mar. 1977.

[5] K. Okada, K. Hashimoto, T. Shibata, and Y. Nagaki, "Optical cable fault location using correlation technique," *Electron. Lett.*, vol. 16, pp. 629-630, July 1980.

[6] K.-I. Aoyama, K. Nakagawa, and T. Itoh, "Optical time domain reflectrometry in a single-mode fiber," *IEEE J. Quantum Electron.*, vol. QE-17, pp. 862-868, June 1981.

[7] M. Nakazawa, T. Tanifuji, M. Tokuda, and N. Uchida, "Photon probe fault locator for a single-mode optical fiber using an acousto-optical light deflector," *IEEE J. Quantum Electron.*, vol. QE-17, pp. 1264-1269, July 1981.

[8] L. Stensland and G. Borak, "Raman time domain reflectometry," in *Tech. Dig. IOOC*, San Francisco, CA, Apr. 1981, p. 104.

[9] K. Noguchi, Y. Murakami, K. Yamashita, and F. Ashiya, "52-km-long single-mode optical fiber fault location using the stimulated Raman scattering effect," *Electron. Lett.*, vol. 18, pp. 41–42, Jan. 1982.
[10] Y. R. Shen and N. Bloembergen, "Theory of stimulated Brillouin and Raman scattering," *Phys. Rev.*, vol. 137, 6A, pp. 1787–1805, Mar. 1965.
[11] T. Miya, A. Kawana, Y. Terumuma, and T. Hosaka, "Fabrication of single-mode fibers for 1.5 μm wavelength region," *Trans. IECE Japan*, vol. E63, pp. 514–519, July 1980.
[12] C. Lin, L. G. Cohen, R. H. Stolen, G. W. Tasker, and W. G. French, "Near-infrared sources in the 1–1.3 μm region by efficient stimulated Raman emission in glass fibers," *Opt. Commun.*, vol. 20, pp. 426–428, Mar. 1977.
[13] D. Gloge, "Weakly guiding fibers," *Appl. Opt.*, vol. 10, pp. 2252–2258, Oct. 1971.
[14] R. H. Stolen, "Nonlinear properties of optical fibers," in *Optical Fiber Telecommunication*, S. E. Miller and A. G. Chynoweth, Eds. New York: Academic, 1972, pp. 125–149.
[15] D. Marcuse, "Loss analysis of single-mode fiber splices," *Bell Syst. Tech. J.*, vol. 56, pp. 703–718, May–June 1977.
[16] R. G. Smith, "Optical handling capability of low-loss fibers as determined by stimulated Raman and Brillouin scattering," *Appl. Opt.*, vol. 11, pp. 2489–2494, Nov. 1972.
[17] R. H. Stolen, E. P. Ippen, and A. R. Tynes, "Raman oscillation in glass optical waveguides," *Appl. Phys. Lett.*, vol. 20, pp. 62–64, Jan. 1972.

Yasuji Murakami (M'79), for a photograph and biography, see p. 586 of the April 1982 issue of this TRANSACTIONS.

Kazuhiro Noguchi was born in Niigata Prefecture, Japan, on September 5, 1955. He received the B.S. and M.S. degrees in applied physics from Tokyo Institute of Technology, Tokyo, Japan, in 1978 and 1980, respectively.

In 1980 he joined the Ibaraki Electrical Communication Laboratory, Nippon Telegraph and Telephone Public Corporation, Ibaraki, Japan, where he has been engaged in research and development on the submarine optical fiber cable, especially on its fault location technique.

Mr. Noguchi is a member of the Institute of Electronics and Communication Engineers of Japan.

Fumihiro Ashiya was born in Tokyo, Japan, on March 6, 1948. He received the B.S. and M.S. degrees in electrical engineering from Waseda University, Tokyo, Japan, in 1971 and 1973, respectively.

When he joined the Ibaraki Electrical Communication Laboratory, Nippon Telegraph and Telephone Public Corporation, Ibaraki, Japan, in 1973, he was engaged in the research of accurate dielectric measurement method for coaxial cable dielectrics. He was later engaged in development of submarine coaxial cables for the wide-band system. He studied core extrusion condition designing, attenuation characteristic designing, and cable loss aging analysis. Recently, he has been engaged in the development of submarine optical fiber cables. Currently, he is the Staff Engineer of the Outside Plant Development Division.

Mr. Ashiya is a member of the Institute of Electronics and Communication Engineers of Japan and the Institute of Electrical Engineers of Japan.

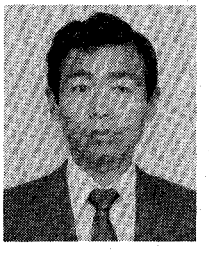

Yukiyasu Negishi graduated from Tohoku University in 1964.

In 1964 he joined the Electrical Communication Laboratory, Nippon Telegraph and Telephone Public Corporation, Ibaraki, Japan, where he has been engaged in research on cable high frequency properties and submarine coaxial cable design. He is presently Chief of the Cable and Material Section, Outside Plant Development Division, Ibaraki Electrical Communication Laboratory.

Mr. Negishi is a member of the Institute of Electronics and Communication Engineers of Japan.

Nobuya Kojima (M'79), for a photograph and biography, see p. 586 of the April 1982 issue of this TRANSACTIONS.